Numerical simulations of accumulated stimulated photon echoes

Vries, Harmen de; Wiersma, Douwe A.

Published in:
The Journal of Chemical Physics

DOI:
10.1063/1.446761

Publication date:
1984

Numerical simulations of accumulated stimulated photon echoes

Harmen de Vries and Douwe A. Wiersma

Department of Physical Chemistry, State University, Nijenborgh 16, 9747 AG Groningen, The Netherlands
(Received 11 February 1983; accepted 29 June 1983)

A theory has been developed describing probe pulse-detected accumulated stimulated photon echo experiments on inhomogeneously broadened electronic transitions. This theory gives a more quantitative description of these experiments than the theory previously developed by Hesselink and Wiersma [J. Chem. Phys. 75,4192(1981)]. At the same time, the present theory provides numerical instead of analytical results. A better founded insight is obtained in the possibilities and limitations of the accumulated photon echo method. The main conclusion is that the measured echo decay curves are still expected to give T_2 directly, thus maintaining the value of the accumulated echo technique as a convenient method to determine picosecond dephasing times. It is concluded that the probe pulse detected accumulated echo method is not readily applied to accurate determinations of intersystem crossing yields.

I. INTRODUCTION

Fairly recently, a new picosecond photon echo technique was developed in the study of dephasing in mixed molecular crystals,[1] utilizing the well-known fact that the lowest triplet state spin sublevels act as population bottlenecks in the optical pumping cycle. It was called the accumulated three-pulse stimulated echo technique (ACC3PSE). The ACC3PSE is closely related to the recently described long-living (anomalous) three-pulse stimulated echo (An3PSE) effect[2,3] appearing in the same energy level system. In both cases, a ground state population grating is created which is converted into an optical echo polarization. However, in an ACC3PSE experiment, the sample is excited by a continuous train of low intensity pulse pairs. In this way gradually a population builds up in the intermediate (triplet) level and a ground state grating of increasing modulation depth develops until a steady-state situation sets in. In this situation, the first pulse of a pair induces the (accumulated) echo appearing at the time of the second pulse of that pair. An important difference between both echo methods is that in ACC3PSE the only convenient variable is t_{12} (the intrapair interval) while in (An)3PSE t_{23} (the interval between the second and third excitation pulses) is varied.

As described by Hesselink[4] and by Hesselink and Wiersma,[1,5] the ACC3PSE method can be used to perform picosecond T_2 (homogeneous dephasing time) measurements as well as to obtain values for kinetic parameters concerning the bottleneck levels. In the present work, specifically, the ACC3PSE method will be considered where the echo is detected in the direction of the probe pulse. Up to now, the probe pulse detected ACC3PSE method has already generated new insight into a number of picosecond dephasing processes.[1,4-8] This method indeed is a promising way to study picosecond and even subpicosecond relaxation processes such as dephasing of electronic and vibronic states in mixed molecular crystals over extended temperature ranges, low temperature fast (~1 ps) vibronic relaxation, relaxation (dephasing) of electronic states of impurity molecules embedded in amorphous host matrices at a few degrees K (glasses,[9-12] polymers,[11,13] and low temperature relaxation in pigment chromophores.[14,15]

To fully exploit the aforementioned possibilities of the ACC3PSE method, it is desirable to work out a theory that accurately accounts for these experiments. The foundation of a correct theoretical treatment was laid by Hesselink and Wiersma.[5] They showed that in the probe pulse detected ACC3PSE method the echo phenomenon is more properly described as a transparency effect than as a burst of coherent radiation. Note that due to the presence of a bottleneck level in this "steady-state" experiment already a measurable transparency can be obtained with small pulse areas ($\ll \pi$). The excitation conditions typical of this technique are taken into account in their theory, namely, the use of small pulse areas and excitation by a train of pulse pairs. However, their theoretical treatment starts from a number of assumptions that in practice often will not be fulfilled. They further do not consider the region $t_{12} \lesssim T_2'$ (t_{12} is the pulse separation within a pair, T_2' is the inhomogeneous dephasing time), while this region is accessible experimentally. In this region, the free induction decay (FID) polarization induced by the first (pump) pulse of the pair can be expected to contribute to the measured signal thereby setting a lower limit to the range of T_2 values that can be determined. With the limitations just mentioned, an analytical expression[5] could be derived that can be directly compared to the ACC3PSE signal measured. This result [Eq. (33) of Ref. 5] reads

$$S(t_{12}) = \frac{I_{on} - I_{off}}{I_{off}} \approx \alpha_{eff} \left\{ \frac{\Theta_1^2}{2} (\gamma + 1) + \Theta_1^2 \gamma \exp(-2t_{12}/T_2) \right\} l \,, \tag{1}$$

S denotes the relative probe beam intensity. Experimentally, the difference between the probe beam intensity with the pump on (I_{on}) and off (I_{off}) is measured as a function of t_{12}. α_{eff} is the effective absorption coefficient, Θ_1 is the pump pulse area, γ is a parameter containing the bottleneck kinetic quantities, and l denotes the sample length. Applying experimental conditions such that Eq. (1) holds, the decay of the transient part of $S(t_{12})$ thus yields T_2, while from the value of $S(\infty)$, an unknown bottleneck kinetic quantity may be determined.

An extensive application of the probe pulse detected ACC3PSE method is to be expected, it is important to know the consequences of not fulfilling experimentally

 0021-9606/84/020657-10$02.10

the conditions for Eq. (1) to hold. In the present work, we will try to solve this problem. Will the decay of the transient part still easily yield T_2? What will be the consequence for the value of a bottleneck kinetic quantity obtained using a more sophisticated theory instead of Eq. (1)? Is a significant FID contribution theoretically expected in the region $t_{12} \lesssim T_2'$? When the limiting conditions for which the theory of Ref. 5 applies are largely removed, an analytical expression for the probe pulse detected ACC3PSE decay curve can no longer be derived. Instead, numerical simulations will be required to interpret the experimentally obtained curves.

In Sec. II, our numerical approach is described where the application of square excitation pulses as well as of Gaussian ones is considered. In Sec. II C the pump pulse propagation is treated. By means of simulations in Sec. III A the question is addressed of whether, with our more sophisticated theory, the ACC3PSE method can still be expected to yield T_2 easily. The parameter values used in these simulations concern the pentacene in naphthalene (PTC/NAPHT) mixed crystal system. The FID region ($t_{12} \lesssim T_2'$) as well as the situation of strong inhomogeneous broadening ($T_2' \ll \tau$, where τ is the FWHM of the excitation pulses) is studied. The value of the ACC3PSE method in determining intersystem crossing (ISC) yields is investigated in Sec. III B. For PTC/NAPHT a comparison is made with ISC results obtained with different methods.

II. PROBE PULSE DETECTED ACC3PSE THEORY

A. Excitation by square pulses

As mentioned above, the present work is a direct continuation of the analytical theoretical efforts by Hesselink and Wiersma.[5] As we also start from the basic framework of their theory, this will be shortly indicated here using Fig. 1. τ is the duration of pump and probe pulses. t_{12} and T are the field-free intra- and interpair intervals, respectively. A pump pulse starts at t_0, a probe pulse starts at t_2^- and ends at t_2^+. The probe pulse interacts with a part of the ACC3PSE polarization, as indicated in the figure. During a pulse pair population, relaxation is neglected, so that one effectively deals with a two-level system that can be described by the u-, v-, w-equations of motion. In this way, the treatment is considerably simplified. On the other hand, this implies the limitation to considering situations where (homogeneous) dephasing occurs much faster than population relaxation. Between the pulse pairs, population relaxation within the appropriate level system is dealt with using a kinetic analysis of the diagonal density matrix elements. These considerations are indicated in the upper part of Fig. 1.

Our first task is to derive the elements of a *generally* valid excitation matrix *including dephasing* (compare Ref. 5, Eq. (3), where it should be noted that a printing error has occurred in the matrix element (2, 2): the term in this element containing the phase factor α_i should be $-\frac{1}{2}\Theta^2 \cos^2 \alpha_i$). These elements E_{ij} are defined according to

$$u(t) = E_{11}u(0) + E_{12}v(0) + E_{13}w(0) , \tag{2a}$$

$$v(t) = E_{21}u(0) + E_{22}v(0) + E_{23}w(0) , \tag{2b}$$

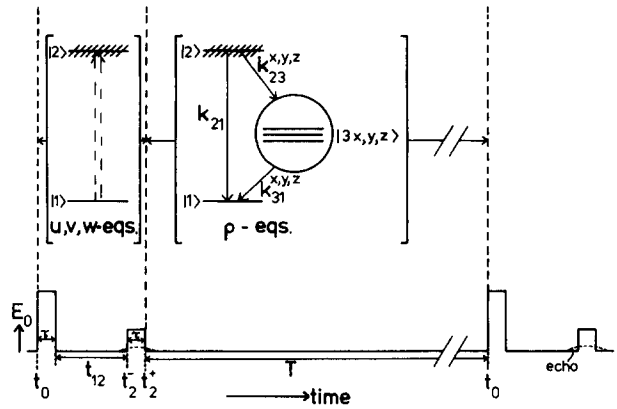

FIG. 1. Probe pulse detected ACC3PSE pulse sequence. The upper part of the figure shows the level schemes used to describe the experiment during the time intervals indicated. $|1\rangle$ is the singlet ground state S_0, $|2\rangle$ is the first excited singlet state S_1 and $|3x, y, z\rangle$ denotes the set of the lowest triplet state spin sublevels $T_1^{x,y,z}$. The shading of level $|2\rangle$ indicates dephasing. The part within the circle has a greatly magnified ($\sim 10^4$) energy scale.

$$w(t) = E_{31}u(0) + E_{32}v(0) + E_{33}w(0) . \tag{2c}$$

$u(0)$, $v(0)$, and $w(0)$ are the initial values (at the beginning of an excitation pulse) of u, v, and w, respectively. We start from the Bloch-like equations of motion

$$\dot{u} = -\Delta v + w\chi_i \sin\alpha_i - (u/T_2) , \tag{3a}$$

$$\dot{v} = \Delta u + w\chi_i \cos\alpha_i - (v/T_2) , \tag{3b}$$

$$\dot{w} = -v\chi_i \cos\alpha_i - u\chi_i \sin\alpha_i , \tag{3c}$$

with the familiar connection to the density matrix elements

$$\begin{aligned} u &= \tilde{\rho}_{12} + \tilde{\rho}_{21} , \\ v &= i(\tilde{\rho}_{21} - \tilde{\rho}_{12}) , \\ w &= \rho_{22} - \rho_{11} . \end{aligned} \tag{4}$$

In this theory, the optical electric field E as a function of the time t for the (linearly polarized) quasimonochromatic plane-wave square excitation pulses is described according to

$$E = E_0 \cos(\Omega_c t - \alpha) \quad (0 \le t \le \tau) , \tag{5a}$$

$$E = 0 \qquad (t < 0 \text{ or } \tau < t) . \tag{5b}$$

E_0 is the constant amplitude during the pulse of length τ. Ω_c is the central frequency (rad s^{-1}) of the Fourier transformed spectrum of this pulse. The "phase factor" is equal to $\alpha = \mathbf{k}\cdot\mathbf{r} - \phi$, where $\mathbf{k}$ and ϕ are the wave vector and the phase, respectively. The detuning of an isochromat with transition frequency ω is given by $\Delta = \Omega_c - \omega$ (rad s^{-1}). The on-resonance Rabi frequency is equal to $\chi = \mu E_0/\hbar$ where μ is the electric dipole matrix element of the pumped transition. The subscript i in Eqs. (3) refers to the pump ($i = 1$) or the probe pulse ($i = 2$). Note that the transformation to the rotating frame has been made according to $\tilde{\rho}_{12} = \rho_{12}\exp(-i\Omega_c t)$ thus maintaining in the equations the individual phase factors α_i.[5] We obtained straightforward solutions of Eqs. (3) by Laplace transformation. This gives formal relations for

the excitation matrix elements. These relations are used in the computer programs so that the effect of the excitation matrix can be calculated in any specific case.

By applying the excitation matrices for the pump and the probe pulse as well as the matrix giving the development of the Bloch vector components during the field-free period t_{12}, the population inversion at the end of the probe pulse can be expressed as

$$w(t_2^*) = p w(t_0) , \tag{6}$$

which is crucial in this ACC3PSE theory. The excitation parameter p is equal to

$$\begin{aligned} p = {}^2E_{31}\exp(-t_{12}/T_2)\{{}^1E_{13}\cos\Delta t_{12} - {}^1E_{23}\sin\Delta t_{12}\} \\ + {}^2E_{32}\exp(-t_{12}/T_2)\{{}^1E_{13}\sin\Delta t_{12} + {}^1E_{23}\cos\Delta t_{12}\} \\ + {}^2E_{33}\,{}^1E_{33} , \end{aligned} \tag{7}$$

where for the excitation matrix elements, a left superscript was added (1 for a pump pulse or 2 for a probe pulse). Using Eq. (6), an expression for the steady-state value of $w(t_0)$ as a function of p and all kinetic parameters can be derived in a similar way as done in Ref. 5, except that in the present work all three triplet spin sublevels are included.

The expressions obtained for p and $w(t_0)$ are needed in the calculation of the interaction between a probe pulse and the accumulated echo polarization. The development of the area of the probe pulse along its propagation direction z is described by Eq. (15) of Ref. 5. This formula contains the Bloch vector component v' in the more familiar rotating frame obtained by the transformation

$$\tilde{\rho}_{12}' = \rho_{12}\exp\{-i(\Omega_c t - \alpha)\} .$$

Performing the integral over the probe pulse duration $\int_\tau v'\,dt$ (in a similar way as done in Ref. 5) and taking a normalized Gaussian distribution for the inhomogeneous function $g(\Delta)$ results in

$$\frac{\partial\Theta_2}{\partial z} = \alpha' \frac{2}{\chi_2\delta\omega_G}\sqrt{\frac{\ln 2}{\pi}}\int_{-\infty}^{+\infty}({}^1E_{33} - p)w(t_0)\exp\left(-\frac{4\Delta^2\ln 2}{\delta\omega_G^2}\right)d\Delta . \tag{8}$$

Here the quantity α' is defined as $\alpha' \equiv \Omega_c N\mu^2/2\hbar\epsilon_0 nc$, where N is the density of the guest molecules, ϵ_0 is the electric permittivity of free space, n is the index of refraction of the host material and c is the velocity of light. Further, $\delta\omega_G$ is the FWHM (rad s^{-1}) of the inhomogeneous distribution. Remember that in Eq. (8) ${}^1E_{33}$, p and $w(t_0)$ all depend on Δ. In the present work, this integration is performed as a numerical summation. After this summation has been carried out, we are left with a relation of the following form

$$\frac{\partial\Theta_2}{\partial z} = F(\Theta_2, z) . \tag{9}$$

This first order differential equation is solved numerically applying the Runge–Kutta method.[16] This results in a value for the probe pulse area $\Theta_2(l)$ at the end of the sample. Then the cycle averaged intensity during the probe pulse and behind the sample is calculated according to

$$I = \tfrac{1}{2}c\epsilon_0 E_{\rm ext}^2 = \frac{c\epsilon_0\hbar^2}{2\mu^2}\left(\frac{3}{n^2+2}\right)^2\frac{1}{\cos^2\zeta}\frac{\Theta_2^2}{\tau^2} , \tag{10}$$

where the Lorentz local field approximation has been applied. $E_{\rm ext}$ is the external field leaving the sample. An angle ζ can exist between the exciting laser field polarization and the direction of μ. Finally, a value is obtained for the relative probe beam intensity

$$S(t_{12}) = \frac{I_{\rm on} - I_{\rm off}}{I_{\rm off}} ,$$

that can be compared to the experimental result. Note that the area Θ of a (pump or probe) pulse having just entered the crystal is obtained from the average intensity $I_{\rm av}$ of the incoming beam using the relation

$$\Theta = \frac{n^2+2}{3}\frac{\mu}{\hbar}\sqrt{\frac{2I_{\rm av}T\tau}{c\epsilon_0}}\cos\zeta . \tag{11}$$

In the present work, the pulse propagation through the sample is treated as follows. First, consider the probe pulse interfering with the echo polarization. During the Runge–Kutta procedure [Eq. (9)] the sample is divided up into a number of slices. At the end of a slice, the area Θ_2 is determined from the field equation [Eq. (15) of Ref. 5] using the Bloch vector components which were calculated using the Θ_2 value at the beginning of that slice. In the Runge–Kutta procedure, the number of slices was adjusted so that the final result no longer significantly depended on this number. This assures a self-consistent treatment of the probe pulse propagation. Now consider the pump pulse propagation. As the repetition period is made to satisfy $T \gg T_2$, when a pump pulse arrives at the sample we have $u(t_0) = v(t_0) = 0$. When furthermore, during the ACC3PSE experiment the condition $\rho_{22} \ll \rho_{11}$ remains valid, there is no need to treat the pump pulse propagation self-consistently. This was assumed to be the case in the present treatment; in other words, the fluorescence lifetime of level $|2\rangle$ is assumed not to be too long compared to T. Then the pump pulse propagation can be treated as is done in Sec. II C. Note the contrast with the usual two pulse, large angle situation studied by Olson *et al.*[17]

The approximations still underlying the theory just presented are:

(a) The fluorescence lifetime of level $|2\rangle$ is assumed to be short enough compared to T, so that a self-consistent treatment of the pump pulse propagation is not necessary;

(b) the echo field is assumed to be much smaller than the exciting probe field. Then the periods t_{12} and T can be considered as being completely field free;

(c) the condition $T \gg T_2$, which can easily be satisfied in practice;

(d) population relaxation during a pulse pair is neglected. This has the important implication of limiting the applicability of the theory to situations where $T_2 \ll T_1$ (T_1 denotes the population relaxation time from the two levels coupled by the radiation field);

(e) in this subsection still square excitation pulses are considered. It should be emphasized that the present theoretical treatment is not limited to situations where $\tau < T_2'$ [we define[18]: $T_2' = \pi g(0)$] or to optically thin samples (see also Sec. II C). Another important im-

provement is the inclusion of dephasing (T_2) during the pulses.

B. Gaussian pulse excitation

It is important to investigate the influence upon our theoretical ACC3PSE results of taking a different and probably more realistic pulse shape, for instance a Gaussian shape. In this context, it is of interest to consider the work of Cooper *et al.*[19] who in optical nutation calculations obtained different results considering square or Gaussian pulse shapes. To allow a numerical treatment of the problem, a Gaussian pulse may be considered as a histogram as a function of time. The question is whether it will still be possible to derive an equation like Eq. (6), which is a prerequisite in order to express $w(t_0)$ as a function of p and all kinetic parameters only, and thus to be able to draft a steady-state theory as done above. It turns out that in the present case such a treatment indeed is possible. The pulses are divided up as shown in Fig. 2. The width of one slice is δt and the slices are numbered from the beginning of the pulse under consideration. A Gaussian curve connects the top centers of the slices. The pulse field has a FWHM of $\delta\tau\sqrt{2}$, where $\delta\tau$ is the FWHM of the pulse intensity. At the base, a pulse field width is chosen of three times the FWHM as indicated in the figure.

Again results like Eqs. (6) and (7) can be derived. However, now the excitation parameter p contains elements of the excitation matrices ${}^1P$ and ${}^2P$ instead of ${}^1E$ and ${}^2E$. Here ${}^1P$ is the product of the excitation matrices of the successive slices constituting the pump pulse. Similarly, ${}^2P$ describes the probe pulse.

In treating the interaction of the probe pulse with the accumulated echo polarization, the starting point is that Eq. (15) of Ref. 5, describing the change with z of the pulse area, holds for each time slice of the pulse separately:

$$\frac{\partial\Theta_{2m}}{\partial z}=\alpha'\int_{-\infty}^{+\infty} g(\Delta)\left(\int_{\delta t_{2m}^-}^{\delta t_{2m}^+} v_m'(\Delta,z,t)dt\right)d\Delta\ , \tag{12}$$

where the subscripts $2m$ denote slice m of pulse 2. The evaluation of the time integral in this equation is somewhat more complicated compared to the square pulse case. Here, it has to be performed numerically as the inversions $w(\Delta,z,\delta t_{2m}^+)$ and $w(\Delta,z,\delta t_{2m}^-)$ at the end and at the beginning of slice m, respectively, cannot simply be expressed in terms of $w(\Delta,z,t_0)$. After that, for each slice the inhomogeneous integration (summation) of Eq. (12) can be performed, and for the complete probe pulse one obtains

$$\frac{\partial\Theta_2}{\partial z}=\sum_m\frac{\partial\Theta_{2m}}{\partial z}=F(\Theta_2,z)\ . \tag{13}$$

This equation is solved applying the Runge–Kutta method resulting in the probe pulse area $\Theta_2(l)$ at the end of the sample. Then the total probe pulse energy density behind the sample can be calculated:

$$E=\frac{c\epsilon_0\hbar^2}{2\mu^2\delta t}\left(\frac{3}{n^2+2}\right)^2\frac{\{\Theta_2(l)\}^2}{\cos^2\zeta}\frac{\sum_m\epsilon_m^2}{\left(\sum_m\epsilon_m\right)^2}\ , \tag{14}$$

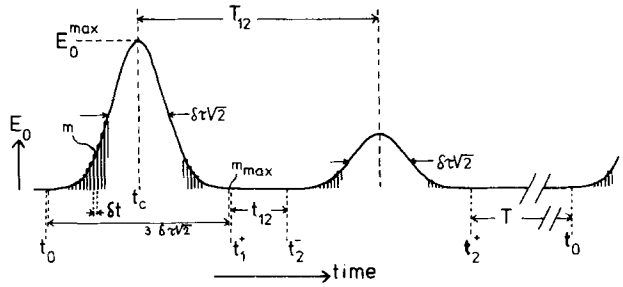

FIG. 2. Histogram-shaped excitation pulse pair applied in the Gaussian pulse ACC3PSE simulations. The electric field amplitude E_0 is drawn as a function of time.

where

$$\epsilon_m=\exp\left[-\frac{2\{(m-\frac{1}{2}m_{max}-\frac{1}{2})\delta t\}^2\ln 2}{\delta\tau^2}\right]\ . \tag{15}$$

The final result is a theoretical value for the relative probe beam intensity

$$S(t_{12})=\frac{E_{on}-E_{off}}{E_{off}}\ . \tag{16}$$

Note that considering Gaussian pulses the area of a pulse having just entered the crystal is obtained from the average intensity of the incoming beam according to

$$\Theta=\frac{n^2+2}{3}\frac{\mu}{\hbar}\sqrt{\frac{2I_{av}T\delta\tau}{c\epsilon_0}\left(\frac{\pi}{\ln 2}\right)^{1/2}}\cos\zeta\ . \tag{17}$$

In the present subsection, temporal overlap of the excitation pulses forming a pair has not yet been considered. However, with Gaussian pulses to study, e.g., the interaction of the probe pulse with the FID polarization induced by the pump pulse often would require to take into account temporal pulse overlap. From preliminary calculations, it can be concluded that this situation also can be treated with a numerical theory. The appropriate equations of motion are easily derived. But the treatment of the probe pulse-echo polarization interaction becomes more complicated compared to the nonoverlap case. This treatment also would include the artifact coherent coupling.[20] Within the scope of the present work the situation of a temporally overlapping pulse pair was not worked out in further detail.

Note that, in fact, any functional curve may connect the slice centers of the temporal pulse histogram. Thus, when the experimental pulse shape would be known from a measurement, e.g., using a streak camera, this actual shape could be taken into account theoretically.

C. The pump pulse propagation

In Sec. II A it was mentioned why in the ACC3PSE experiments considered here the pump pulse propagation does not have to be treated self-consistently. However, the sample optical density (OD), causing $\Theta_1(z)$ to decrease for increasing values of z, should be taken into account. Since in solving Eq. (9) using the Runge–Kutta method in the z direction the sample is divided up into a number of slices, it is possible *after* each slice to correct the pump pulse area for the absorption *by* that slice. In the analytical theory of Ref. 5 such a $\Theta_1(z)$ correction is in-

corporated far less simply, especially when the sample has a considerable OD.

As long as the absorption coefficient $\alpha(\omega)$ remains unchanged, use can be made of the spectrally integrated pulse intensity $\bar{I}(z)$:

$$\bar{I}(z) = C^N \int_{-\infty}^{+\infty} I^N(0,\omega)\exp[-\alpha(\omega)z]\,d\omega \ , \tag{18}$$

where Beer's law has been applied. For PTC/NAPHT the low intensity absorption coefficient is given by[21,22]

$$\alpha(\omega) = \frac{\pi\omega N g(\omega)\ \mu^2\cos^2\xi}{cn\epsilon_b\hbar} \ , \tag{19}$$

where ϵ_b is the electric permittivity within the naphthalene crystal for b-polarized light. The normalized spectral distribution function of the pulse approaching the sample is $I^N(0,\omega)$, while C^N is a normalization factor. In an ACC3PSE experiment at the moment the pump pulse arrives, a steady-state population grating is present, the shape of which depends on t_{12} (or T_{12}) as well as on z. Therefore, Eq. (18) should be applied to each Runge–Kutta sample slice separately. Since in the present situation, we have to deal with a considerably depleted ground state, the absorption coefficient should contain an effective (saturated) inhomogeneous distribution function (Ref. 18, Chap. 6). Thus, for the first slice we take

$$\alpha^{(1)}(\omega) = -\bar{\alpha}g(\omega)w(\omega,h,t_0) \ , \tag{20}$$

where the inversion at the end of the slice (thickness h) is used. The quantity $\bar{\alpha}$ is obtained from $\alpha(\omega)$ [Eq. (19)] by omitting the inhomogeneous function $g(\omega)$ and replacing ω by Ω_c. For the PTC/NAPHT example considered in this work the value $\bar{\alpha} = 2.05\times10^{14}\,\mathrm{s^{-1}\,m^{-1}}$ was determined using a measurement of the low intensity probe pulse transmission with the pump beam blocked. Using Eq. (20) the pump pulse intensity transmitted by M sample slices is found to be described by

$$\frac{\bar{I}_1(Mh)}{\bar{I}_1(0)} = \int_{-\infty}^{+\infty} I^N(0,\omega)\exp\left\{\bar{\alpha}g(\omega)h\sum_{U=1}^{M} w(\omega,Uh,t_0)\right\}d\omega \ . \tag{21}$$

Thus, within the Runge–Kutta loop for sample slice number M the population grating $w(\omega, Mh, t_0)$ at the end of that slice is calculated. This result is used to obtain the pump pulse area $\Theta_1(Mh)$, which is taken to be proportional to $\{\bar{I}_1(Mh)\}^{1/2}$ and which is the area entering the next slice. The assumption underlying this treatment is that in traversing the sample, the pump pulse is considered to retain its original (input) shape as a function of time, with a (peak) intensity equal to that of the more correctly shaped pulse corresponding to the Fourier transform of $I(z,\omega)$. Finally note here that we take into account the full convolution of Beer's exponential function with the input spectral intensity distribution. Therefore, the present treatment, in principle, can handle data from ACC3PSE experiments where the pulse duration is $\gtrsim T_2'$ as well as from experiments on high OD samples. This last point is very important considering the acquisition of good ACC3PSE signals, which often will require samples with appreciable absorption.[4]

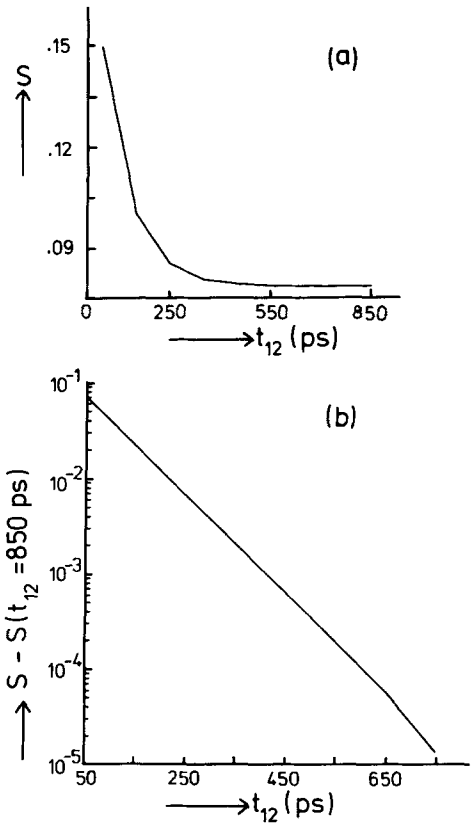

FIG. 3. (a) ACC3PSE decay obtained in a square pulse simulation applying PTC/NAPHT parameters as discussed in the text. Here $T_2 = 172$ ps. The signal S was calculated for nine values of the pump–probe pulse interval t_{12} increasing from 50 up to 850 ps in 100 ps steps. In this figure the calculated points are connected by straight lines. (b) Semilogarithmic plot of the quantity $\{S - S(t_{12} = 850\ \mathrm{ps})\}$ obtained in the same simulation showing the functional behavior of the ACC3PSE signal decay.

III. SIMULATION RESULTS

A. Obtaining T_2 with the ACC3PSE method

1. A practical case

One of the main questions of this work is whether, within the present more sophisticated theory, the usefulness of the probe pulse detected ACC3PSE as a method to measure dephasing times can be confirmed. In this section the inhomogeneous FID after the pump pulse will first be left out of consideration. In other words the situation $t_{12} \gtrsim T_2 > T_2'$ will be studied. Simulations were performed for the PTC/NAPHT-case experimentally studied by Hesselink and Wiersma.[4,5]

First consider a simulation with square excitation pulses applying a pulse length $\tau = 25$ ps. Further parameter values of interest here are $T_2 = 172$ ps, the inhomogeneous FWHM is $\delta\nu_G = 30$ GHz or $\delta\bar{\nu}_G = 1\ \mathrm{cm^{-1}}$, and the intrapair field-free period t_{12} runs from 50 to 850 ps with steps of 100 ps. The resulting (S, t_{12}) plot is shown in Fig. 3(a). It looks similar to the experimentally obtained signal curves,[1] consisting of a decaying part on top of a constant background, as is also concluded from the theory of Ref. 5. The logarithmic plot of the quantity $\{S - S(t_{12} = 850\ \mathrm{ps})\}$ against t_{12} is shown in Fig. 3(b).

A straight line results extending over nearly four decades. The slight deviation at the end is caused by plotting $\{S - S(t_{12} = 850 \text{ ps})\}$ instead of $\{S - S(\infty)\}$. It can be concluded that the ACC3PSE curve of Fig. 3(a) indeed obeys

$$S(t_{12}) = A + Be^{-Ct_{12}} . \tag{22}$$

Comparing this to Eq. (1) the question arises whether $C = 2/T_2$. This was carefully checked and it turned out indeed to be the case within numerical error limits (within 1%). Further, it is interesting to note that under appropriate conditions ($\tau \ll T_2$, low sample OD) our square pulse simulation program yields nearly identical results as compared to the theory of Hesselink and Wiersma[5]: an identical T_2-value, a B/A-value 1.2% less and a value for the constant background $S(\infty)$ being 0.7% less. This is a gratifying result. As a next test, simulations were performed with the Gaussian pulse program under conditions fairly like those used to produce Fig. 3. This also resulted in an ACC3PSE behavior obeying Eq. (22), with $C = 2/T_2$.

Thus, from the simulations discussed so far it can be concluded that the ACC3PSE method is still theoretically expected to be very convenient for an accurate T_2 determination. Additional results on this point are discussed further on.

To demonstrate the steady-state ground state depletion in an ACC3PSE experiment, two grating plots are shown of the steady-state inversion $w(t_0)$ as a function of the detuning. Figure 4 shows a grating obtained in a square pulse simulation for $t_{12} = 125$ ps under otherwise the same conditions used to produce Fig. 3. Note that just the inversion is plotted and thus no convolution with the inhomogeneous distribution $g(\Delta)$ is included. Note that the expected side bands on both sides of the main

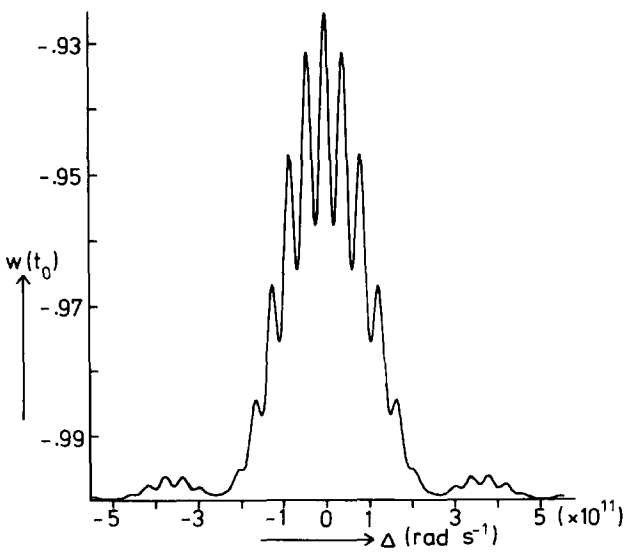

FIG. 4. Steady-state inversion $w(t_0)$ in the sample input plane ($z = 0$) as a function of the detuning. The inversion grating was obtained in a square pulse simulation under the same parameter conditions used to produce Fig. 3. Specifically, $t_{12} = 125$ ps, while the total ISC yield was taken to be 0.9%.

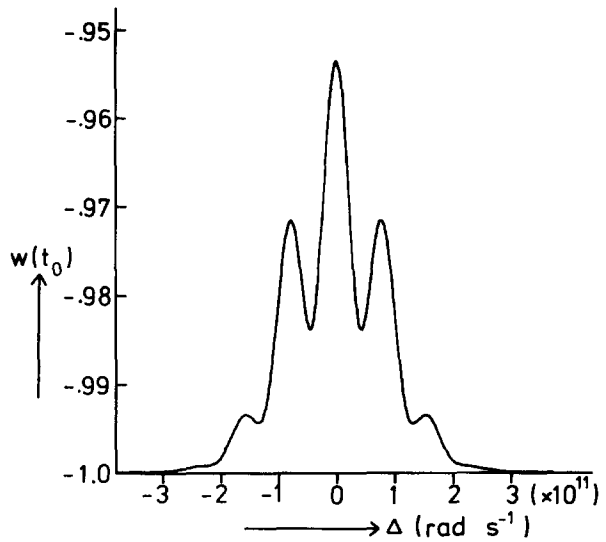

FIG. 5. Steady-state inversion $[w(t_0)]$ grating obtained in a Gaussian pulse simulation. In this case, $T_2 = 172$ ps, $T_{12} = 75$ ps, and the total ISC yield equals 0.36%.

band of the pulse spectral distribution simply appear upon applying the excitation matrices. It can be seen that in this case with a total ISC yield of 0.9% at line center $w(t_0) > -0.93$. Figure 4 reveals a grating period of 41.3 GHz rad. Putting this equal to $2\pi/t$, it follows that $t = 152$ ps. Thus, the grating period is determined by the time $t_{12} + \tau = 150$ ps between the pump and probe pulse centers rather than by the field-free interval t_{12}. The latter fact might be expected from simple 3PSE theory.[23] An inversion grating resulting from a Gaussian pulse simulation with $T_2 = 172$ ps and $T_{12} = 75$ ps is shown in Fig. 5. Again just $w(t_0)$ is plotted here for $z = 0$. Now, with a total ISC yield of 0.36% at line center we have $w(t_0) \approx -0.953$. From Fig. 5 a grating period can be derived of 78.1 GHz rad, yielding a time t of 80.4 ps. This is even larger than T_{12}, while here $t_{12} = 10.1$ ps.

It will be clear now that in such an ACC3PSE experiment the interval between pump and probe pulse has to be scanned slowly compared to $1/k_{31}$ (as this is the longest time in the system kinetics) to enable the steady-state grating to establish itself each time anew. For longer intervals t_{12} the signal will become increasingly more sensitive to spectral diffusion processes which might occur, as because of the decreasing grating period, the grating itself is destroyed more easily.

2. *The FID region*

When in the analytical theory of Ref. 5 one allows t_{12} values in the range $t_{12} \lesssim T_2'$, this results in complicated terms representing contributions to the probe pulse transmission from the inhomogeneous FID polarization induced by the pump pulse. However, the theory given in the present work easily allows t_{12} to take on values in the range $t_{12} \lesssim T_2'$. Such calculations were performed for the practical PTC/NAPHT case considered above, where $T_2 \gg T_2'$ ($T_2 = 172$ ps). It is important here to distinguish between square pulse excitation and excitation by Gaussian pulses as upon using Gaussian ones with $\delta\tau$

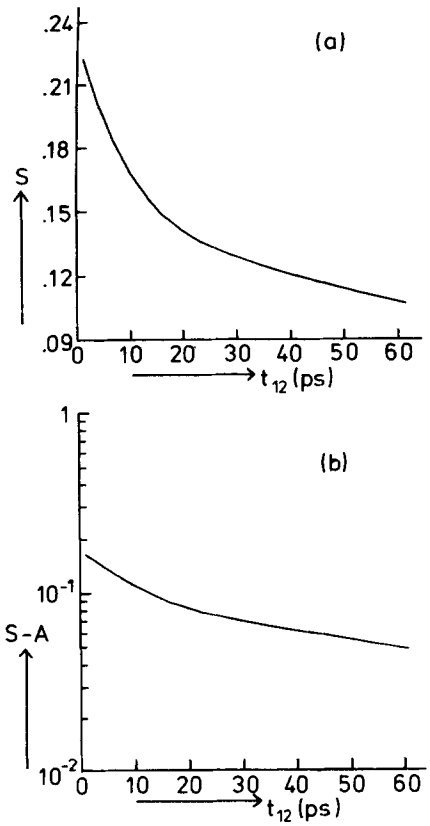

FIG. 6. (a) Square pulse simulated ACC3PSE decay during the first 60 ps of the pump–probe pulse interval t_{12} for the PTC/NAPHT parameter set of Fig. 3. The wave vector was expressed as $|\mathbf{k}| = 2\pi n_b/\lambda_{air}$. (b) Semilogarithmic plot of the quantity $(S-A)$ showing the distinct FID contribution in the decay curve in the (a) part of this figure.

$\approx T_2'$ the FID contribution cannot be well studied theoretically, in connection with the fact that temporal pulse overlap is left out of consideration (Sec. II B).

Consider a square pulse FID simulation using similar parameter values as those leading to Fig. 3, thus $\tau = 25$ ps, while $T_2' = 15.7$ ps. The resulting ACC3PSE signal for t_{12} ranging from 1 to 61 ps is shown in Fig. 6(a). The concomitant logarithmic plot of the quantity $\{S(t_{12}) - S(\infty)\}$ is shown in Fig. 6(b). This latter plot does show an FID contribution to the signal for t_{12} values up to 28 ps. This should be compared to the experimental result that no convincing indication was found for an FID contribution.[1,4,6] To be able to judge the significance of the difference between these theoretical and experimental results, an additional number of calculations was performed.

In the simulation of Fig. 6, the index of refraction of the NAPHT host material was taken into account in the value of the wave vector ($n = 1.72$ for b-polarized light[24]). When this is just left out of consideration the plots shown in Fig. 7 are obtained. The FID part of the signal has increased by nearly a factor of 10 while the stimulated echo part is unaffected. This can be explained since the FID polarization is arrayed optimally in the direction of the pump pulse, while it is probed at an angle φ. Then for a longer wavelength upon traversing the sample, the phase difference between the pump and the probe pulse will be smaller, thus giving an increased probe pulse detected FID polarization. But as the echo polarization is arrayed along the probe pulse direction, its contribution to the signal will remain unaffected. It can be concluded that the FID contribution is very sensitive to changes in n and therefore in the presently studied case to the polarization of the light relative to the NAPHT b axis.

Another square pulse simulation was performed with $\tau = 2$ ps. This short pulse excitation turned out to decrease the general signal level considerably while the FID contribution lasts to longer t_{12} values. A Gaussian pulse simulation with $\delta\tau = 2.3$ ps showed a more pronounced FID contribution compared to the $\tau = 2$ ps case. From further simulations it became apparent that the FID part of the signal is sensitive to the angle φ between pump and probe beams, to the sample length l and to the area ratio Θ_1/Θ_2.

The FID contribution was theoretically shown to depend on several parameters. Moreover, in the ACC3PSE experiments done so far, a number of excitation parameter values were rather uncertain. A simulation using a set of parameter values close to the ones in a particular PTC/NAPHT experiment showed a rather small FID contribution (Fig. 6). Thus, the absence of an experimental FID signal under these conditions can be ac-

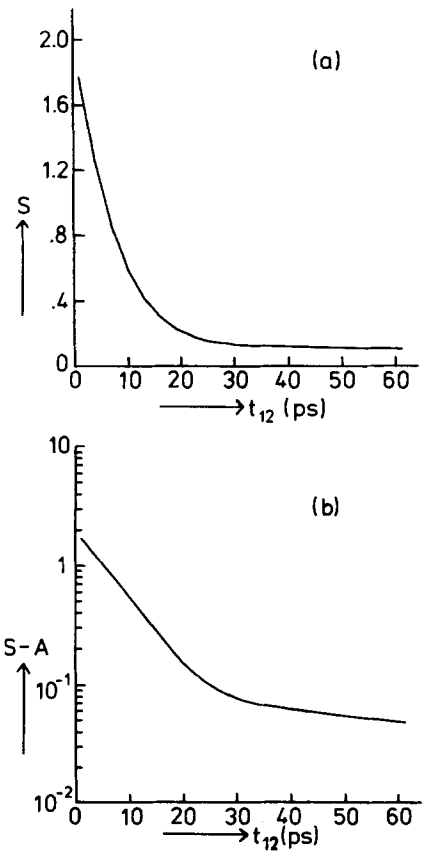

FIG. 7. Results of a simulation similar to the one of Fig. 6, except that now the wave vector is expressed as $|\mathbf{k}| = 2\pi/\lambda_{air}$.

counted for by the theory developed in this work. However, in general, when performing an ACC3PSE experiment one should be aware of a potential FID contribution to the signal, especially when studying a case where $T_2 \lesssim 2T_2'$.

For a case with a large FID contribution, a series of simulations was performed with different T_2 values leading to the conclusion that in such a case the ACC3PSE method can still be used to measure T_2 values satisfying $T_2/T_2' \gtrsim 2$. The decays then directly give T_2 as it was checked that in these cases again $C = 2/T_2$ [Eq. (22)]. For $T_2/T_2' < 2$ the constant intensity $S(\infty)$ did not contain simple information on T_2.

3. Strong inhomogeneous broadening

In this subsection, the situation where $T_2' \ll \tau$ will be considered. This case is of practical interest in view of the study of dephasing in organic glass systems (Refs. 9–12). These systems show a large inhomogeneous broadening (of the order of 100 cm^{-1}) of the electronic transitions of the guest molecules as well as dephasing times which are comparable to the pulse lengths attainable with most of the presently operating picosecond dye laser systems. Of course, in these organic glass samples, one should be aware of the possibility of T_2 variation within the inhomogeneous band.

In the case of strong inhomogeneous broadening, an FID contribution to the ACC3PSE signal might be present, coming from the part of the inhomogeneous band covered by the pulse spectrum. A series of square pulse simulations was performed with $\tau = 10$ ps, an inhomogeneous FWHM of 52 cm^{-1} (or $T_2' = 0.3$ ps), and with T_2 ranging from 30 to 5 ps. These simulations included the region $t_{12} < \tau$. The results did not show any ACC3PSE signal increase due to, e.g., and FID contribution. Applying different pulse shapes, this kind of inhomogeneous FID contribution is expected to last at most up to about one pulse length after the pump pulse. Then, choosing a pulse length $\delta\tau \lesssim \frac{1}{2}T_2$ would enable one to measure T_2 despite the presence of that FID contribution. However, for shorter times ($\delta\tau < 1$ ps) the pulse peak power would have to be raised accordingly to prevent the pulse areas from becoming too small to give measurable ACC3PSE signals. A square pulse simulation of such a high peak power case yielded a single ACC3PSE decay with $C = 2/T_2$ [Eq. (22)]. This result was also obtained in the series of square pulse simulations mentioned above (where T_2/τ ranged from 3.0 to 0.5). Finally, the same result was obtained in a "glass" simulation with the Gaussian pulse program, where the parameters were $\delta\tau = 2.3$ ps, $T_2 = 5$ and $T_{12} \geq 11$ ps. Thus, in principle, the ACC3PSE method is expected to be very suitable to the study of dephasing in, for instance, organic glass systems.

It is finally of interest here to report that the series of square pulse simulations mentioned above shows an increase of the constant background signal [the A part of Eq. (22)] from 0.047 for $T_2 = 5$ ps up to 0.084 for $T_2 = 30$ ps. This can be explained from the fact that when T_2/τ does not exceed too much the value of 1, during excitation various molecular polarizations contributing to any isochromat vector in the rotating frame irreversibly rotate in a horizontal plane and thus more or less withdraw themselves from the population excitation process. This would cause $A = S(\infty)$ to increase for longer T_2 values. Note that this effect could show up here since in the present theory we do take into account dephasing during excitation. As for the FID simulations of Sec. III A 2 also in this glass situation no simple relationship emerged between A and T_2.

B. Obtaining ISC yields with the ACC3PSE method

In Ref. 5 it was emphasized that kinetic feeding or decay parameters of the bottleneck levels could be quantitatively determined from ACC3PSE results. Here this will be considered more closely based on our numerical theory. A number of PTC/NAPHT simulations was performed using parameter values that applied to ACC3PSE experiments carried out by Hesselink. Most of these values were not determined very accurately as the experiments were primarily meant to yield T_2 instead of the $|2\rangle \rightarrow |3\rangle$ ISC rate.[25] We used the spin sublevel populating probabilities and decay rates of the lowest triplet state determined by Van Strien and Schmidt.[26] Note that the value of 280 μs for the Z spin sublevel decay obtained with the well established method of Ref. 26 is the most reliable one. Using this value while applying the present ACC3PSE theory does not lead to unrealistic ISC values. This solves the apparent discrepancy concerning the value of τ_z.[5]

Square pulse simulations were performed varying the pulse width, the sample optical density and the input pulse areas within their respective ranges that applied to the experiment. The values of $S(\infty)$ thus obtained were compared to the experimental one. This resulted in a range of PTC/NAPHT singlet $\rightarrow$ triplet ISC yield values between 1% and 12%. A corresponding series of Gaussian pulse simulations yielded ISC values between 0.4% and 2.5%. Thus, these simulation results vary over nearly two orders of magnitude. This variation would be eliminated by simulating an accurately performed ACC3PSE experiment (including a precise pulse shape and width determination). However, it has to be noted here that even then, the result would have to be considered with reserve. In the first place, the local optical electric field cannot be accurately determined with any method known so far. The other important point here is a consequence of the condition $T_2 \ll T_1$ mentioned at the end of Sec. II A. Mostly because of this condition, the ACC3PSE experiment will have to be performed at temperatures well above 1 K in order to make meaningful comparisons with our theory. In that case, it should be recognized that the radiationless rate constants, e.g., in the PTC level system, may be temperature dependent. Especially, it is likely that spin-lattice relaxation between the triplet spin sublevels will not be negligible. As this process is not included in our theory, this is the other reason why the precise simulation result just mentioned should be considered with reserve.

It is of interest to compare the presently obtained PTC/NAPHT ISC results with those determined with different techniques. First, reconsider the OFID experiment reported in Ref. 22. Combining the result of that

experiment with the triplet spin sublevel kinetic values obtained in Ref. 26 leads to an ISC yield $<5.5\%$ which is compatible with our present results.

The PTC/NAPHT ISC rate at low temperature was also studied by Lambert and Zewail[27] measuring transient fluorescence signals.[28] They reported an ISC yield of the order of 0.3% but remarked that their actual numbers were not very accurate. Moreover, in the derivation of the theoretical formulas used in their analysis, the inhomogeneous broadening was not treated correctly.[22,29]

Recently in our laboratory the PTC/NAPHT ISC was also studied utilizing the An3PSE effect.[2,3] From a fit to the experimentally obtained decay using the triplet parameters of Ref. 26 the ISC yield was concluded to be $15\pm3\%$. This is distinctly higher than our ACC3PSE simulation results. Note here that the An3PSE theory[2,3] was based on the assumptions of resonant excitation ($\Delta=0$) and negligible decay during the pulses. Both conditions were not strictly met in the experiment. However, compared to the other methods discussed, the An3PSE method has the important advantage that knowledge about the local optical electric field is not required. Moreover, this method can be applied for temperatures of ≈1 K, where spin-lattice relaxation within the triplet manifold can be neglected mostly.

The main conclusion here is that the probe pulse detected ACC3PSE method is less suited for an accurate ISC determination. In most cases the An3PSE technique[2,3] should be preferred where care should be taken that the experimental and theoretical conditions agree. Still it remains justified to conclude that the ISC yield in PTC/NAPHT considerably exceeds that in PTC in p-terphenyl (lower sites).[22,29]

Finally, the simulations mentioned above showed the constant signal value $S(\infty)=A$ to be directly proportional to the ISC yield provided the remaining parameter values are kept fixed (including T_2!). Therefore, in a number of cases, observed A values might be utilized to determine relative ISC yields, e.g., for the four sites of PTC in p-terphenyl when the other parameter values are all similar for these sites. We further like to note here that our ACC3PSE simulations yielded values for the signal ratio B/A in the range of 0.3 up to 3.0, strongly dependent on, among others, the pulse shape, the pulse width and T_2. This corrects the expectation from the less sophisticated theory of Ref. 5 that $B/A=2.0$ ($\gamma\gg1$, $\Theta_1\ll1$).

IV. CONCLUSIONS

A theory, including numerical methods, describing probe pulse detected ACC3PSE experiments was constructed, starting from the theoretical framework of Hesselink and Wiersma.[5] Considering the usefulness of the present theory, the following points are important. In calculating the pulse areas from the input beam intensities the Lorentz local field approximation is used. Our theory allows the sample to be optically thick which is especially important considering ACC3PSE experiments. The theory does not suffer from limitations to the ratio τ/T_2' (the spectral width of the pulse compared to the inhomogeneous width) or to the ratio t_{12}/T_2' (thus including the FID region). Dephasing during the pulses is taken into account as well as the presence of three intermediate triplet spin sublevels. In principle, our treatment can handle excitation pulses of any temporal shape.

Under appropriate limiting conditions the present theory results in values of T_2, B/A and $S(\infty)=A$ similar to those of the theory of Ref. 5 (within $\approx1\%$). For a wide range of physically important parameters, our simulations show that the main conclusion of Ref. 5 is not affected: the measured ACC3PSE decay curves are expected to yield T_2 directly, as the signal is found to obey the relation

$$S(t_{12})=A+B\exp(-2t_{12}/T_2)\,. \tag{23}$$

In such experiments the t_{12}-scan velocity should be low enough to enable the steady-state grating to establish itself each time anew. For longer intervals t_{12} one should be increasingly aware of possibly occurring spectral diffusion processes.

From a study of the region where $t_{12}\approx T_2'$ it is concluded that the presently lacking experimental evidence of an FID contribution can be accounted for by the theory developed in this work. However, generally one should be aware of a potential FID contribution to the ACC3PSE signal. If such a contribution does appear, T_2 values can be measured when $T_2/T_2'\gtrsim2$.

Also the situation of strong inhomogeneous broadening ($T_2'\ll\tau$) was studied. The ACC3PSE method is concluded to be very suitable to dephasing studies in this situation (organic glass systems). The quantity $A=S(\infty)$ is found to increase upon lengthening T_2.

The applicability of the ACC3PSE method in order to determine ISC yields quantitatively was studied. Square pulse simulations of a preliminary ACC3PSE experiment on PTC/NAPHT by Hesselink[25] yielded ISC values in the range of 1% to 12%. From comparable Gaussian pulse simulations, ISC yields resulted lying between 0.4% and 2.5%. In the course of this work, we were able to explain the discrepancy apparently existing between the τ_e values determined by Hesselink and Wiersma[1,5] and by Van Strien and Schmidt.[26]

It was concluded that the probe pulse detected ACC3PSE method is less suited for an accurate ISC determination. In most cases, the An3PSE technique[2,3] should be preferred.

Finally, we want to make some remarks on the application of the ACC3PSE method to vibronic transitions, as was done with the mixed crystals PTC/NAPHT[6,7] and PTC/p-terphenyl.[7] Experimentally, it was checked that in this situation the ACC3PSE decay also gives T_2, by comparison with a vibronic 2PE result.[6] To describe the vibronic experiment theoretically, the level scheme contains an additional level. Moreover, in this case the condition $T_2\ll T_1$ no longer applies and population relaxation during a pump–probe pulse pair has to be taken into account. Therefore, a theoretical description of a vibronic ACC3PSE experiment will be more complex than the theory developed in the present work.

For the interested reader, a preliminary but considerably more detailed version of this article is available on request at the above address.

ACKNOWLEDGMENTS

We are indebted to Dr. D. P. Weitekamp for critical perusal of the manuscript. The investigations were supported by the Netherlands Foundation for Chemical Research (S. O. N.) with financial aid from the Netherlands Organization for the Advancement of Pure Research (Z. W. O.).

[1]W. H. Hesselink and D. A. Wiersma, Phys. Rev. Lett. **43**, 1991 (1979).
[2]J. B. W. Morsink, Thesis, University of Groningen, 1982.
[3]J. B. W. Morsink, W. H. Hesselink, and D. A. Wiersma, Chem. Phys. **71**, 289 (1982).
[4]W. H. Hesselink, Thesis, University of Groningen, 1980.
[5]W. H. Hesselink and D. A. Wiersma, J. Chem. Phys. **75**, 4192 (1981).
[6]W. H. Hesselink and D. A. Wiersma, J. Chem. Phys. **73**, 648 (1980).
[7]W. H. Hesselink and D. A. Wiersma, J. Chem. Phys. **74**, 886 (1981).
[8]K. Duppen, L. W. Molenkamp, J. B. W. Morsink, D. A. Wiersma, and H. P. Trommsdorff, Chem. Phys. Lett. **84**, 421 (1981).
[9]J. M. Hayes, R. P. Stout, and G. J. Small, J. Chem. Phys. **74**, 4266 (1981).
[10]G. J. Small, in *Spectroscopy and Excitation Dynamics of Condensed Molecular Systems*, edited by V. M. Agranovich and R. M. Hochstrasser (North–Holland, Amsterdam, 1983), Vol. 4, p. 515.
[11]F. Drissler, F. Graf, and D. Haarer, J. Chem. Phys. **72**, 4996 (1980).
[12]J. Friedrich and D. Haarer, Chem. Phys. Lett. **74**, 503 (1980).
[13]E. Cuellar and G. Castro, Chem. Phys. **54**, 217 (1981).
[14]J. Friedrich, H. Scheer, B. Zickendraht-Wendelstadt, and D. Haarer, J. Chem. Phys. **74**, 2260 (1981).
[15]J. Friedrich, H. Scheer, B. Zickendraht-Wendelstadt, and D. Haarer, J. Am. Chem. Soc. **103**, 1030 (1981).
[16]E. Kreyszig, *Advanced Engineering Mathematics*, 3rd ed. (Wiley, New York, 1972).
[17]R. W. Olson, H. W. H. Lee, F. G. Patterson, and M. D. Fayer, J. Chem. Phys. **76**, 31 (1982).
[18]L. Allen and J. H. Eberly, *Optical Resonance and Two-Level Atoms* (Wiley, New York, 1975).
[19]D. E. Cooper, R. W. Olson, R. D. Wieting, and M. D. Fayer, Chem. Phys. Lett. **67**, 41 (1979).
[20]E. P. Ippen and C. V. Shank, in *Ultrashort Light Pulses*, edited by S. L. Shapiro (Springer, Berlin, 1977), Vol. 18, p. 83.
[21]R. Loudon, *The Quantum Theory of Light* (Clarendon, Oxford, 1973).
[22]H. de Vries and D. A. Wiersma, J. Chem. Phys. **70**, 5807 (1979); **71**, 5389(E) (1979).
[23]R. L. Shoemaker, in *Laser and Coherence Spectroscopy*, edited by J. I. Steinfeld (Plenum, New York, 1978), p. 197.
[24]K. S. Sundararajan, Z. Kristallogr. **93**, 238 (1936).
[25]W. H. Hesselink (private communication).
[26]A. J. van Strien and J. Schmidt, Chem. Phys. Lett. **70**, 513 (1980).
[27]Wm. R. Lambert and A. H. Zewail, Chem. Phys. Lett. **69**, 270 (1980).
[28]H. de Vries, Ph. de Bree, and D. A. Wiersma, Chem. Phys. Lett. **52**, 399 (1977); **53**, 418(E) (1978).
[29]T. E. Orlowski and A. H. Zewail, J. Chem. Phys. **70**, 1390 (1979).